Journal of Physics: Condensed Matter

TOPICAL REVIEW

# Nano-plasmonic antennas in the near infrared regime

To cite this article: N Berkovitch *et al* 2012 *J. Phys.: Condens. Matter* **24** 073202





IOP Publishing Journal of Physics: Condensed Matter
J. Phys.: Condens. Matter **24** (2012) 073202 (16pp) doi:10.1088/0953-8984/24/7/073202

TOPICAL REVIEW

# Nano-plasmonic antennas in the near infrared regime

**N Berkovitch**[1], **P Ginzburg**[2] **and M Orenstein**[1]

[1] Department of Electrical Engineering, Technion, Haifa 32000, Israel
[2] Physics Department, King's College, London, UK

E-mail: nikolaib@tx.technion.ac.il

Received 9 September 2011, in final form 8 November 2011
Published 6 January 2012
Online at stacks.iop.org/JPhysCM/24/073202

**Abstract**
Plasmonic nano-antennas constitute a central research topic in current science and engineering with an enormous variety of potential applications. Here we review the recent progress in the niche of plasmonic nano-antennas operating in the near infrared part of the spectrum which is important for a variety of applications. Tuning of the resonance into the near infrared regime is emphasized in the perspectives of fabrication, measurement, modeling, and analytical treatments, concentrating on the vast recent achievements in these areas.

(Some figures may appear in colour only in the online journal)

## Contents

1. Introduction 1
2. Fabrication and measurements of plasmonic nano-antennas 2
   2.1. Fabrication of plasmonic nano-antennas 2
   2.2. Measurements of plasmonic nano-antennas 2
3. Theory—analytical solutions 4
4. From visible to near infrared 5
   4.1. Shifting resonances to the NIR by geometrical aspect ratios 5
   4.2. Coupling 5
   4.3. Concavity 7
   4.4. Particle shape design by evolutionary algorithms 8
   4.5. Substrate of the nano-antenna 9
5. Applications of plasmonic nano-antennas 10
   5.1. Receiver mode 10
   5.2. Transmission mode 11
   5.3. Enhancement of quantum and nonlinear phenomena 11
6. Future outlook and conclusion 12
   Acknowledgments 12
   References 12

## 1. Introduction

The interaction of high-frequency electromagnetic fields with noble metal objects is referred to as plasmonics. The use of this extraordinary interaction may be traced back as far as the Bible [1], where a prescription for preparing a liquid metamaterial consisting of water and gold nanoparticles can be found. Later and even before Newton's first law was formulated [2], similar phenomena were used by ancient masters—small metal particles of different sizes produce a variety of colors that may be observed in stained glass all over the world today. However, comprehensive studies of plasmonic phenomena, connecting theoretical predictions with existing experiments, seemingly started at the middle of the 20th century. Usually, it is convenient to distinguish between propagating and localized surface plasmons; however, both originate from the combination of light–plasma interactions and the interface between negative and positive dielectric response of plasmonic materials at certain frequencies.

As a milestone in the research on propagating plasmons it is remarkable to point to the works of Wood [3] in 1902 where anomalous diffraction from metal gratings was discovered. The existence of surface plasmons was first predicted in 1957 by Ritchie [4]. In 1959 Powell and Swan [5]

 

demonstrated that electron beams may have an additional channel of energy loss, corresponding to the creation of surface plasmons. In 1968 Ritchie *et al* connected the phenomena of surface plasmons with Wood's anomaly [6]. In the same year experimental verification, using optical excitation assisted by prism coupling, was performed by Kretschmann and Raether [7] and subsequently by Otto [8]. Localized plasmons, as already mentioned, were known about long ago, but the first theoretical analysis was performed by Lorentz [9] and then by Mie in 1908 [10]. Excitation of resonances of small metal particles was demonstrated by Kreibig and Zacharias [11] in 1970. Starting from the first surface enhanced Raman spectroscopy (SERS) experiment [12], detection and sensing using plasmonic particles has motivated the recent interest in the field.

The main macroscopic difference of the noble metals from other dielectric objects at optical and near infrared (NIR) frequencies is a negative dielectric response, namely a negative real part of the electrical permittivity ($\varepsilon$). Relying on this fact, metal–dielectric layers may support unique modes called surface plasmon polaritons (SPPs) which may be confined in one or two dimensions and guided by plasmonic waveguides or even localized in all three dimensions by metallic nanoparticles in the sub-wavelength regime. The rebirth of plasmonics a decade ago was started by a vast interest in guided SPP modes [13, 14] that were expected to constitute the next generation photonic circuitry with a possible reduction of the size from the micron to the nanometric scale. Additionally, since energy flows in opposite directions at negative/positive $\varepsilon$ boundaries, it results in slow phase (and group) velocity of the plasmonic modes and consequently in a possibility of sub-wavelength confinement. SPP modes, being tightly confined to boundaries, may go beyond the diffraction limit of the exciting light, as shown both theoretically and experimentally in adiabatic conical metal rods [15] and tapered [16–18] or abrupt impedance-matched metal/insulator/metal (MIM) waveguides [19]. However, because of the relatively high Ohmic losses of the highly confined SPPs, they cannot be guided for large distances, limiting the applicability of SPP circuitry such that integrated/hybrid plasmonic/dielectric components should be used [20, 21]. On the other hand, the research on localized plasmon modes in metallic nanoparticles has increased dramatically due to their ability to concentrate and enhance electromagnetic fields by orders of magnitude and to efficiently scatter electromagnetic radiation even when the size of the metallic particles is much smaller than the wavelength of the excitation field. Based on these characteristics the plasmonic nanoparticles are forming efficient nano-antennas that can operate in the visible and near infrared regimes.

Control of the characteristics (e.g. resonance) of the plasmonic nano-antennas opens the possibility for a variety of practical and prospective applications including enhanced sensing and spectroscopy [22], plasmonic sensors [23] and biosensors [24, 25], cancer imaging and therapy [26, 27], building blocks of metamaterials [28–30], the ability to redirect scattered light [31], plasmonic lasers [32], which can be included in the larger family of SPASERs [33], enhanced nonlinearities [34], enhancement of radiation efficiencies [35], enhancement of the Raman signal (SERS) by orders of magnitude [36, 37], and many more. While most reported resonances of typical plasmonic nano-antenna response are located in the visible spectrum, this review emphasizes the NIR regime, which is an important application field for plasmonics.

## 2. Fabrication and measurements of plasmonic nano-antennas

### *2.1. Fabrication of plasmonic nano-antennas*

The materials generally employed for plasmonic nano-antennas are noble metals—mainly gold and silver—and, more rarely, aluminum [38], composite semiconductor structures [39, 40], and heavily doped semiconductors [41, 42]. The choice of antenna material is one of the key elements in defining its properties, but since the choice of plasmonic materials for the visible and NIR regime is currently very limited, it does not allow enough control over antenna performance. However, due to the dependence of the resonance on the particle's geometry, it is common to tune the plasmon resonance of a nano-antenna by changing the shape and size of the metallic particle. The shapes of the nanoparticles can be defined by self-assembly processes, using chemical methods that control the growth of metal crystals [43–51]. However, despite the large variety of particle shapes achievable by these methods, the resulting particles are characterized by a spread of parameters even within a single sample, and, in addition, single nano-antennas are practically impossible to isolate. The self-assembly method is thus not optimal for systematically studying the dependence of the plasmon resonance on the particle geometry and interparticle spacing. For this purpose, highly engineered nanofabrication techniques such as electron beam lithography (EBL), focused ion beam (FIB) milling, direct laser writing [52], or similar [53, 54] should be used. Employing these methods, homogeneous arrays of nanoparticles may be fabricated with precise control over the particle shapes and interparticle distances [55].

### *2.2. Measurements of plasmonic nano-antennas*

Characterization of the properties of plasmonic nano-antennas may be accomplished in several ways. The simplest is to measure scattering (related transmission and/or reflection) spectra from nano-antennas illuminated by a broadband source (in our case a broadband NIR source). Analysis of the transmission spectrum allows determination of the resonance wavelength primarily of the dipole mode that strongly interacts with the far field excitation. Moreover, for more complex-shaped antennas, such as coupled nanoparticles, shift of the resonance wavelength relative to that of an isolated single-particle antenna can teach us about the particles' mutual interaction. Additional information may be extracted from the spectral measurements on the polarization

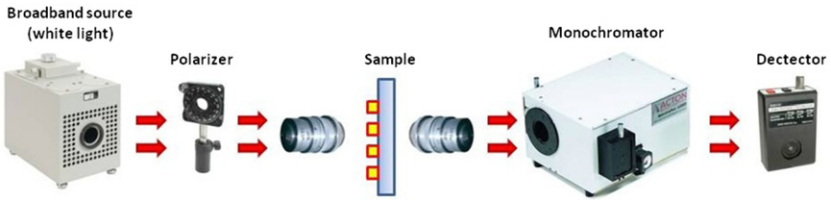


**Figure 1.** The scheme of the setup for measuring the normal incidence transmission spectrum.

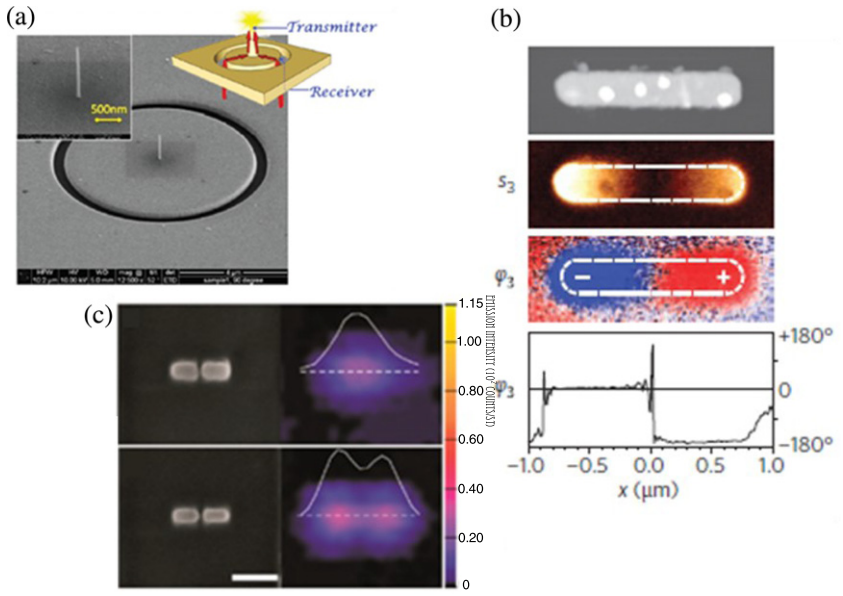


**Figure 2.** Measurements of a single antenna: (a) excitation of a nanopillar by a plasmonic ring aperture (reproduced with permission from [58]. Copyright 2011 American Chemical Society); (b) NSOM mapping of near field intensity and phase in a nanorod (reproduced with permission from [61]. Copyright 2009 Macmillan Publishers Ltd); (c) two-photon photoluminescence of coupled plasmonic particles (reproduced with permission from [62]. Copyright 2010 American Chemical Society).

dependence of the nano-antenna interactions. This can be measured by adding a polarizer to the setup to measure the spectral response for different polarization states. A typical configuration for measuring the normal incidence transmission spectrum is shown in figure 1.

This setup includes a broadband light source, a polarizer (optional), an imaging system that illuminates the sample and collects the signal scattered in the forward direction, a monochromator, and a detector. The output of such a measurement is the spectrum of the transmitted light with wavelength resolution determined by the gratings of the monochromator and intensity resolution determined by the sensitivity of the detector. Most of the particles have resonance eigen-modes that can be excited by linear polarization, but there are plasmonic nano-antennas that are excitable favorably by vectorial polarization, depending on the antenna symmetry—e.g. radial and azimuthal polarization states [56, 57].

A method enabling high contrast (signal to background) measurement of a single nano-antenna requires focusing of the exciting light onto the effective cross section of the nano-antenna under test. This is a rather difficult task due to the small dimensions of nano-antennas. Thus, scattering measurements are in many cases performed on particle arrays rather than on a single nano-antenna. An array configuration with a cell size comparable to the effective cross-section area of the nano-antenna is a favorable solution. Furthermore, one can also monitor the light at its first diffraction order of the array period to enhance further the contrast. It should be noted that the transmission spectral shape consists of contributions from the forward scattering by the nano-antenna, the radiation absorbed by the particle and the array factor (care is usually taken to make the latter small for studying basic antenna effects). A method enabling measurement of a single nano-antenna by employing an additional large plasmonic focusing lens is reported in [58]. In the latter, the impinging illumination is conveniently focused into a few micron diameter plasmonic lens consisting of a small ring-shaped aperture in a thin Au layer (figure 2(a)). The circular ring in this case acts as a receiving plasmonic lens-antenna that transforms radially polarized excitation into a focusing cylindrical SPP on the rear side of the film, where the plasmonic nano-antenna under test (in this case a nano-needle) is located. The forward scattered radiation is finally collected by the large-area detector.

Dark field microscopy can also be used in order to enhance the contrast of measurements for single nano-antennas. In this method the background illumination is not collected by the imaging objective [59, 60].

Although spectral measurements provide substantial information regarding the properties of plasmonic nano-antennas, they do not show the near field distribution in close vicinity to the particles, which is highly important for many applications employing an enhanced field. The electrical field or intensity profile of the plasmon antenna field may be deduced indirectly by comparing the spectral results with numerical simulations that provide both spectral and modal information. Direct optical imaging of the localized plasmon mode is not satisfactory since the features of the near field (intensity) are of a dimension much smaller than the wavelength of the excitation field and thus beyond the resolution of an imaging apparatus.

The most straightforward means of measurement of the near field is to place a small, minimally perturbing receiving optical antenna in the near field of the nano-antenna under test, and measure the intensity profile by means of near field scanning optical microscopy (NSOM) [61, 63]. An example of such a near field measurement is shown in figure 2(b), demonstrating not only the intensity distribution of the electrical field on the nanoparticle, but also mapping its phase [61] by coherent detection techniques. Additional, more exotic techniques have been demonstrated, including nonlinear photoluminescence mapping [62] by two-photon photoluminescence, which strongly correlates with the local intensity of the electrical field enhanced by the antenna resonance (figure 2(c)). A high spatial resolution source may be obtained by a high-energy electron beam generated by a scanning (transmission) electron microscope—S(T)EM. In this case cathodoluminescence is generated from the nanoparticle and collected by the detector [64] or secondary electron emission may be studied in the EELS configuration [65].

The far field spectral measurements described above can also provide the angular emission pattern, by measuring the (spectral) intensity as a function of angle [64]. The directivity (angular dependence) is an important characteristic of the nano-antenna.

## 3. Theory—analytical solutions

The resonance wavelengths of plasmonic nanoparticles may be calculated analytically for certain shapes, e.g. ellipsoids and cylinders, and, in general, for any shapes, which have 'simple' boundaries in coordinate systems, where the Laplacian operator is separable. The solution for the basic spherical shape is known as Mie theory [66]. In the quasistatic limit, when the size of the particles is much smaller than the wavelength of the excitation field, the resonance wavelengths of the field eigen-modes for a spherical metal particle, embedded in a homogeneous dielectric, can be determined using the following equation:

$$\varepsilon_{\mathrm{p}}(\omega) = -\varepsilon_{\mathrm{d}}\frac{N+1}{N} \tag{1}$$

where $\varepsilon_{\mathrm{p}}(\omega)$ is the dielectric constant of the particle, $\varepsilon_{\mathrm{d}}$ is the dielectric constant of the surrounding medium, and $N$ is the mode order: $N = 1$ (dipole), $N = 2$ (quadrupole), etc. Note that, since $\varepsilon_{\mathrm{p}}(\omega)$ describes the dielectric constant of a metallic nanoparticle, it is a complex number; on the other hand, $\varepsilon_{\mathrm{d}}$ generally stands for the dielectric surrounding of the particle and thus it is predominately real. Therefore equation (1) can be fulfilled only approximately. For example, equation (1) for the first order (dipole) mode of a spherical Au nanoparticle with a diameter of 100 nm surrounded by air is obtained in the visible part of the spectrum: $\lambda_0(\mathrm{Au}) = 480$ nm.

As a result of the spherical symmetry, (1) is independent of the polarization of the excitation field which is not the case for particles of other shapes. The resonance conditions for ellipsoidal-like cross sections, such as disks or cylinders, may be found by modifying the condition of equation (1) with a geometrical factor. For the dipole mode this condition will become

$$\varepsilon_{\mathrm{p}}(\omega) = \varepsilon_{\mathrm{d}}\left(1 - \frac{1}{L}\right) \tag{2}$$

where $L$ is the Lorentz depolarization factor [66, 67]. It is a closed form expression for an ellipsoid and is given by the aspect ratio between its major axes. For an ellipsoid there are three different geometrical factors (that determine three different resonances), while for a sphere they degenerate into the single value $L = 1/3$. For a general case, the Lorentz depolarization factor may be estimated empirically using different numerical techniques.

The polarizability of an ellipsoidal particle of volume $V$ in an incident electrical field parallel to a principal axis of the ellipsoid is given by [66]

$$\alpha = V\frac{\varepsilon_{\mathrm{p}}(\omega) - \varepsilon_{\mathrm{d}}}{\varepsilon_{\mathrm{d}} + L[\varepsilon_{\mathrm{p}}(\omega) - \varepsilon_{\mathrm{d}}]}. \tag{3}$$

Thus at the resonance the particle will behave as a dipole with its strength determined by the volume ($V$), shape ($L$), and material properties of the particle and the surroundings ($\varepsilon_{\mathrm{p}}(\omega), \varepsilon_{\mathrm{d}}$). For a given polarizability of the particlethe absorption $C_{\mathrm{abs}}$ and scattering $C_{\mathrm{sca}}$ cross sections can be defined as [66]

$$C_{\mathrm{abs}} = k\,\mathrm{Im}\{\alpha\} \qquad C_{\mathrm{sca}} = \frac{k^4}{6\pi}|\alpha|^2 \tag{4}$$

where $k$ denotes the wave number of the incident electrical field. Both of these cross sections depend on the particle's polarizability $\alpha$ and the wave number but the functional dependences are different. This means that the absorption and scattering efficiencies of the particle will exhibit their maxima at (usually slightly) different wavelengths. In general, for very small nanoparticles (smaller than the penetration length of ~20 nm) the absorption cross section will be dominant, while for larger particles the scattering (radiation resistance) will overcome the absorption, unless dark modes are excited. Another interesting phenomenon can be shown by separating the real and imaginary parts of the particle's permittivity $\varepsilon_{\mathrm{p}}(\omega)$ in equation (4). It can be shown [66] that the maximum absorption is inversely proportional to the absorptive part of the particle's permittivity, which may look counter intuitive. On the other hand, this allows a lossy plasmonic material such as aluminum to be used as the plasmonic nanoparticles, while

in the case of an SPP, aluminum loss, which is much larger than that of gold or silver, will reduce its applicability.

While analytical solutions for resonance frequencies are known only for a small number of particle shapes, numerical methods may be used for design and analysis. Various methods such as the finite difference time domain (FDTD) [68, 69], the finite element method (FEM) [70], the boundary element method (BEM) [71], the T-matrix approach [72], the discrete dipole approximation (DDA) [73], the generalized multiparticle Mie (GMM) theory [74], and more have been employed for this purpose. Each method has its own advantages and disadvantages in terms of complexity, computational efficiency, running time, and accuracy. We refer the interested reader to the cited references and to the survey paper by Myroshnychenko *et al* [75], comparing the most popular computational methods used for modeling of optical responses in nanoparticles.

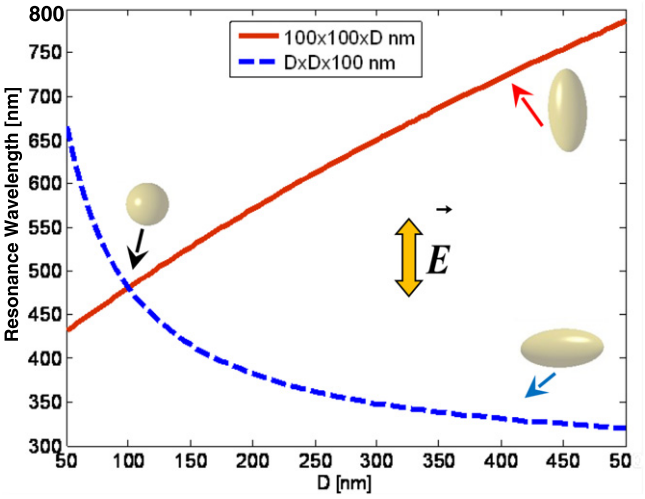


**Figure 3.** Plasmon resonance wavelength dependence on the diameter ($D$) of the ellipsoid particle. The arrow shows the polarization of the excitation field.

## 4. From visible to near infrared

Potential applications of plasmonic nanoparticles in the NIR (0.75–2 $\mu$m) part of the spectrum include, among others, optical communications and biomedical applications. However, in the quasistatic limit, the plasmon resonance of the spherical particle is weakly dependent on size and for most plasmonic materials lies in the visible range. Thus more complicated modifications of the plasmonic nano-antennas are required. We will discuss below major methods that allow the plasmon resonance to be shifted toward the NIR wavelengths.

### *4.1. Shifting resonances to the NIR by geometrical aspect ratios*

Equation (2) depicts the dependence of the resonance wavelength of a metallic ellipsoid on the relative dimensions of the particle and their position in respect to the direction of polarization of the excitation field. It may be shown by equation (2) that alignment of the polarization along the longest axis of an ellipsoid provides maximal red shift of the resonance relative to a spherical particle, while alignment of the polarization along the shortest dimension leads to blue shift. Such a dependence is demonstrated in figure 3 for a Au ellipsoid particle in vacuum by varying the particle's dimensions relative to the polarization of the excitation field (the dispersion characteristics of Au were estimated by the Drude model).

Thus, in order to shift the resonance wavelength of the nanoparticle toward the NIR, the particle's dimension in the direction of the field polarization should be increased or, on the other hand, the particle's dimension in the perpendicular direction should be decreased [76, 77]. This tendency can also be shown by using a quantum mechanical time-dependent density functional theory [78]. Although the use of elongated particles instead of spheres is one of the simplest ways to achieve the red shift of the resonance, it has several disadvantages. First, in order to generate a considerable shift of the resonance (by hundreds of nanometers), particles with a very high aspect ratio are required. Thus the size of the particle in its long dimension tends to be larger than the desired nanometer scale, which make it impossible to use it in applications such as metamaterials, where the unit cells should be much less than the excitation wavelength. Another issue that should be considered is the polarization dependence of the elongated particles. Although it might be beneficial in some cases, in other applications, such as plasmonic enhancement of solar cells, this dependence will be a disadvantage [79, 80].

### *4.2. Coupling*

One of the most common possibilities for shifting the resonance of a plasmonic nano-antenna is to couple several particles. Being coupled, and with the nomenclature taken from chemical bonding, the 'energy levels' (correspondingly the plasmonic resonances) are mixed, creating, in the most simple case, bonding and anti-bonding states with corresponding energies lying below and above the original two-fold degenerate levels of the standalone particles. Thus the bonding configuration of the coupled nanoparticles will be red-shifted relative to the single-particle case with a resonance shift that is determined by the strength of the interaction.

*4.2.1. Hybridization.* The well established hybridization concept, used in chemistry and solid state, may be applied for the description of the resonance behavior of complex structures [81]. Combinations of simple geometries with known standalone solutions (e.g. shell—combination of a sphere with a spherical hole) may be successfully treated, as was shown in [82, 83] and is demonstrated in figure 4. The energy-level diagram of figure 4 shows the split of bonding and anti-bonding states for an interacting spherical particle and spherical cavity.

The bonding state of the nanoshell will be red-shifted relative to the spherical nanoparticle, and by reducing the thickness of the shell, the magnitude of the shift can be significantly increased.

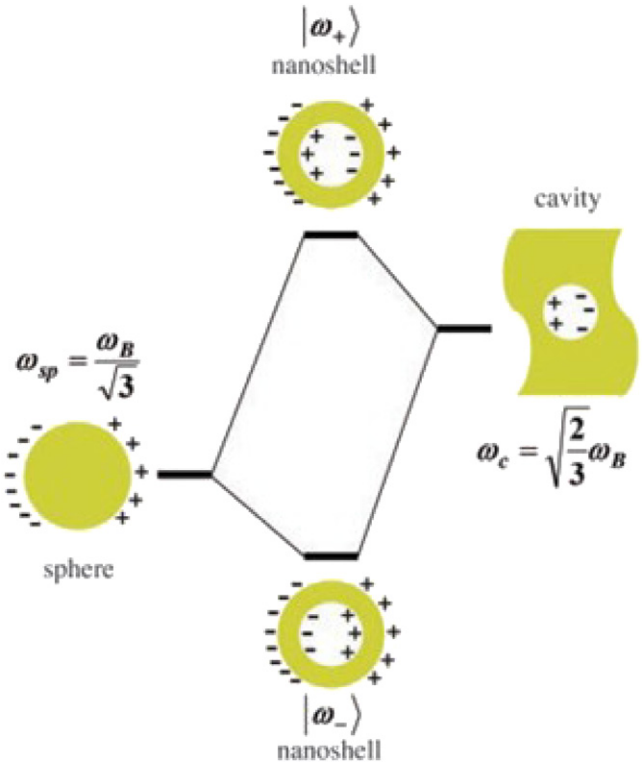


**Figure 4.** An energy-level diagram describing the plasmon hybridization in metal nanoshells resulting from the interaction between a sphere and cavity plasmons. The two nanoshell plasmons are an anti-symmetrically coupled (anti-bonding) $\omega_+$ plasmon mode and a symmetrically coupled (bonding) $\omega_-$ plasmon mode. Reproduced with permission from [82]. Copyright 2003 AAAS.

*4.2.2. Capacitive coupling.* In electrical-engineering terminology, a few coupled nano-antennas may be treated as capacitively, inductively, and conductively coupled nano-circuits. Two main scenarios of the coupled nanoparticles may be considered. In the first scenario the coupled particles are separated by a dielectric material and thus this will be further called the capacitive coupling case. In the second scenario the particles are connected by a conductive medium and this will be considered as a conductive coupling case.

Nanoparticle dimers are the simplest structures to study for the capacitive coupling phenomenon. The spectral response of such dimers differs from the response of single particles and depends also on the spatial separation between the particles and the polarization direction of the excitation field relative to the pair axis. In general, the plasmon resonance has a red shift (that increases with reducing interparticle distance) for parallel polarization and a small blue shift for perpendicular polarization compared to the resonance of the isolated particles.

Some models describe dimer resonance as an interaction between two adjacent oscillating point dipoles. In such models there is an assumption that the external field excites an electrical field in each standalone particle, which is similar to the near field of a point dipole with $1/d^3$ distance dependence, where $d$ is the distance between two adjacent dipoles. The advantage of point dipole models is their extension from simple dimer resonance to resonance and propagating modes in long nanoparticle chains [84]. Such modes can propagate in straight and bent particle chains [85, 86], and the electromagnetic energy transferred by these modes can be measured, e.g. by placing additional fluorescent dye close to the particle chains [87]. The disadvantage of point dipole models is related to their inability to predict resonance wavelengths correctly for all sizes of nanoparticles and gaps. The condition required for the point dipole model is to keep the interparticle gap larger than the diameter of the particles, i.e. weak coupling between particles, otherwise higher multipolar interaction should be taken into account [88]. On the other hand, for particles separated by too large gaps the interaction is not predominantly near field coupling, and correction for retardation effects should also be considered [89, 90].

Another approach to describe the resonance of the dimmer is by means of the well-known tools from the field of radio-frequency antennas. In this model two coupled nanoparticles are treated as a dipole antenna fed at its center, and analysis of the antenna response is described in terms of impedance matching and optical radiation resistance, rather than in terms of scattering and absorption cross sections [91, 92].

Closed chains of nano-antennas are subject to periodical boundary conditions, which may dramatically alter the behavior of such arrays. While for open configurations nearest neighbor coupling describes quite well the mode structure [84], closed systems manifest collective response and even produce considerable magnetic moments at optical frequencies [93]. Analytical expressions have been derived for closed-loop arrays with subsequent explanation of dark modes with suppressed far field radiation [94]. Change of the geometrical properties of individual particles in closed-loop arrays (in analogy to chemical molecules they also may be called oligomers) may dramatically change the resonance behavior of the structures, manifesting a strong signature of collective behavior [95].

Slight changes in local geometry may also be seen as effective coupling between modes of the original structure. Since a variety of collective modes exist in the initial structure and may be coupled by these perturbations, the analogy to quantum effects (having also classical counterparts) such as electromagnetically induced transparency and Fano resonances may be demonstrated [96].

*4.2.3. Conductive coupling.* The transition from the coupled to the touching regime dramatically modifies the resonance behavior [97–99]. When particles are touching, a conductive bridge is formed, thus transferring coupled plasmonic nano-antennas from the capacitive to the conductive coupling regime. The same effect can also be achieved by changing the conductivity of the connecting junction by increasing significantly the free carrier density in the gap between the particles [100, 101]. It is essential, however, to clarify here the 'conductivity' notion. Although conductive coupling, charge transfer dimers, etc are commonly used in this field, due to the similarity of these nano-plasmonic structures to regular circuit elements connected by conductive wire or to charge

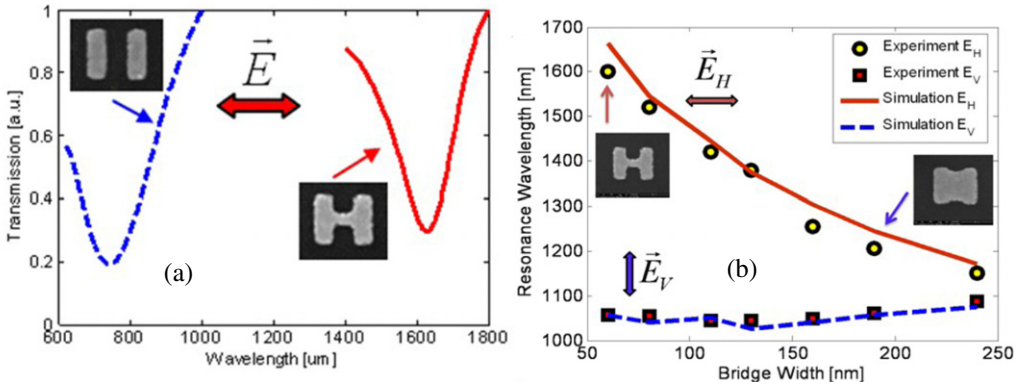


**Figure 5.** (a) Transmission (forward scattering) spectra of the coupled and connected particles; the bold arrow denotes the polarization of the excitation field. (b) Resonance wavelength of the connected particles as a function of the bridge width for horizontal, $E_{\mathrm{H}}$, and vertical, $E_{\mathrm{V}}$, polarizations. Reproduced with permission from [102]. Copyright 2011 American Chemical Society.

transfer molecular complexes, it is important to say that we are not dealing with real conductivity. The metal particles are predominantly dipolar materials at optical frequencies (their losses—real conductivity—are definitely not the main effect determining the resonances). The 'conductive' wire is thus not the equivalent of a DC conductor and the 'current' flowing in the structure is rather a displacement (dipole) current, while the notion of high conductivity here is related to the high absolute value of the material dipole moment (real part of the electric susceptibility). As a consequence, the resonance characteristics after establishing even the tiniest conductive bridge are primarily determined by the ability of the surface charge to redistribute over the surfaces of the whole combined structure. The idea that in the touching regime the particle's behavior, such as resonance location and field enhancement, cannot be explained by a simple theory of coupled particles, but is determined by the geometry of the whole combined particle, was demonstrated experimentally in [102].

For polarization parallel to the interparticle axis the introduction of a narrow (60 nm) conductive wire between the particles abruptly shifts the transmission resonance of the dimer to the NIR part of the spectrum by more than 900 nm (figure 5(a)). It may be thought that by enhancing the 'conductivity' in the gap, namely increasing the wire width, we should expect a further red shift. But, as can be seen in figure 5(b), the inverse effect occurs, and the spectral shift moderates as we enhance the wire width. Since the gap between the particles remains constant, the shift of the resonance wavelength is only due to the substantial redistribution of the surface charge to be much more delocalized—thus contributing to the red shift.

### *4.3. Concavity*

In order to shift the particle's resonance by hundreds of nanometers toward the NIR, extreme modifications of the configurations discussed above are required: coupled particles separated by only several nanometers, few-nanometer-thin nanoshells, or extreme aspect ratio ellipsoids. However, the repeatable fabrication of such configurations is challenging and limits their applicability. Another solution of this problem is to exploit the interaction of the surface charge and the local geometry for the concave structures.

A method that directly connects the surface charge distribution, the local geometry of a particle, and their mutual interactions is based on surface integral equations. In the electro-quasistatic regime the geometry-dependent eigen-solutions for the surface charge density and the eigen-values, related to the resonance frequency, are given by the following Fredholm integral equation of the second kind [103]:

$$\sigma(\mathrm{Q}) = \frac{\varepsilon_{\mathrm{p}}(\omega)-1}{\varepsilon_{\mathrm{p}}(\omega)+1}\oint_S \sigma(M)\frac{\vec{r}_{\mathrm{MQ}}\cdot\hat{n}_{\mathrm{Q}}}{\pi|\vec{r}_{\mathrm{MQ}}|^2}\cdot \mathrm{d}S_M \qquad (5)$$

where $\sigma(\mathrm{Q})$ is the surface charge density at point Q, $\varepsilon_{\mathrm{p}}(\omega)$ is the particle's dispersive dielectric constant, $\vec{r}_{\mathrm{MQ}}$ is a vector, connecting two points on the particle boundaries, any point (M) with a point of interaction (Q), $\hat{n}_{\mathrm{Q}}$ is a normal to the boundary at the point Q, and the integration is performed on the particle boundary. For convex particles, the normal to the surface always points in the direction of the charge separation vector $\vec{r}_{\mathrm{MQ}}\cdot\hat{n}_{\mathrm{Q}} > 0, \forall\,\mathrm{M},\mathrm{Q}$ (figure 6(a)) resulting in Blaschke's topological theorem [103]:

$$\frac{\varepsilon_{\mathrm{p}}(\omega)-1}{\varepsilon_{\mathrm{p}}(\omega)+1} > \frac{1}{1-\frac{A}{4\pi RD}} \qquad (6)$$

where $A$ is the area of a particle, $R$ is the maximum radius of curvature of its boundary, and $D$ is the minimal diameter of the embedding sphere. Dispersion relations for plasmonic metals lead to negative values for $\varepsilon$ ($< -1$) increasing in absolute value with $\omega$, meaning that shift toward NIR frequencies will always be accompanied by significant aspect ratios.

On the other hand, for concave particles (thus not satisfying the relation of equation (6)), the normal to the surface can point in a counter direction to the charge separation vector, resulting in a local negative value of the scalar product within the integrand of equation (5) ($\exists\,\mathrm{M},\mathrm{Q}: \vec{r}_{\mathrm{MQ}}\cdot\hat{n}_{\mathrm{Q}} < 0$), which may yield a reduced value of the resonance frequency whenever a significant surface charge distribution is generated on the concave edges (figure 6(b)). Although equation (5) can be solved only numerically, it gives

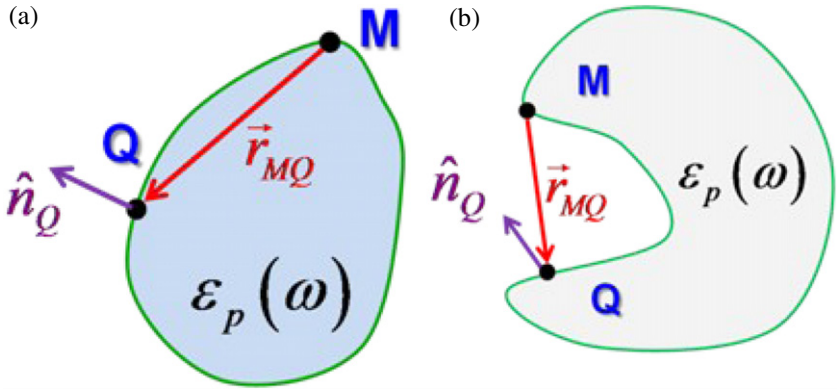


**Figure 6.** Particles of (a) convex and (b) concave shapes.

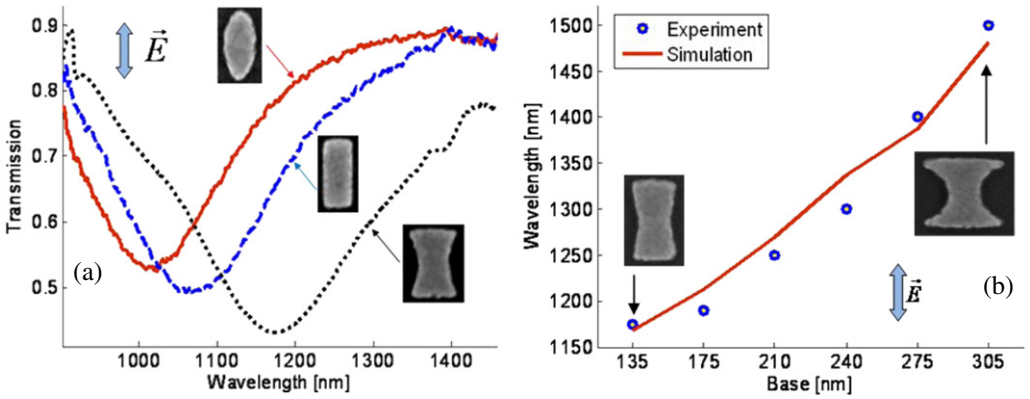


**Figure 7.** (a) Measured transmission spectra of an elliptical disk (red solid line), a rectangle (blue dashed line), and a concave hyperbolic particle (black dotted line). (b) Resonance wavelengths of concave hyperbolic particles plotted as a function of their base-width: measured values (blue rings) and FDTD results (red solid line). The arrow designates the polarization of the incident field. Reproduced with permission from [104]. Copyright 2010 American Chemical Society.

an indication that the concavity of the particle is a parameter that can be used to move the plasmon resonance to the longer wavelengths.

The importance of the concavity parameter was confirmed experimentally in [104], where particles of the same aspect ratio but with different convex/concave cross section were tested. Figure 7(a) shows the transmission spectrum as a function of wavelength for particles with different concavity types: convex, rectangular, and concave. Well defined minima, corresponding to the dipole resonances of individual elements, clearly show the significant red shift of the concave particle with respect to the convex particle, while both have the same dimensional aspect ratio. Moreover, by increasing the 'concavity factor' of the particle its resonance may be widely tuned into the NIR regime without changing the aspect ratio of the particle very much (figure 7(b)). In summary, concavity tuning provides much flexibility (hundreds of nanometers) without the requirement of high aspect ratios and complex lithographical techniques.

It should be noted that even in the case of the concave particle the direction of excitation is still important. In order to benefit from the concavity of the particle the positive and negative charges should be separated along the concave boundary, as is predicted by equation (5).

Another example related to the concave structures is the well-known split ring resonator [105, 106]. For polarization that is parallel to the gap the main dipole mode of the structure is located at long wavelengths which are determined by the length of the whole structure that works as a folded antenna.

### *4.4. Particle shape design by evolutionary algorithms*

As discussed earlier, the shape of the particle is one of the major tools to tune the plasmon resonance. In order to get the required resonance wavelength for a given surroundings the shape of the initial particle is generally modified by variation of one or several geometrical parameters, such as the length of the elongated particle, the concavity factor, etc. The drawbacks of these techniques are currently the technological limits, such as minimal particle size and minimal distance between particles (defined by fabrication possibilities), or maximal antenna length for metamaterial applications, etc.

While evolutionary algorithms of different kinds [107] are widely used in electromagnetic research for optimization of excitation signal for a given shape [108] and for antenna engineering [109], very few have been implemented in the field of nano-plasmonics, for instance the particle-swarm optimization method for field enhancement [110]. Recently,

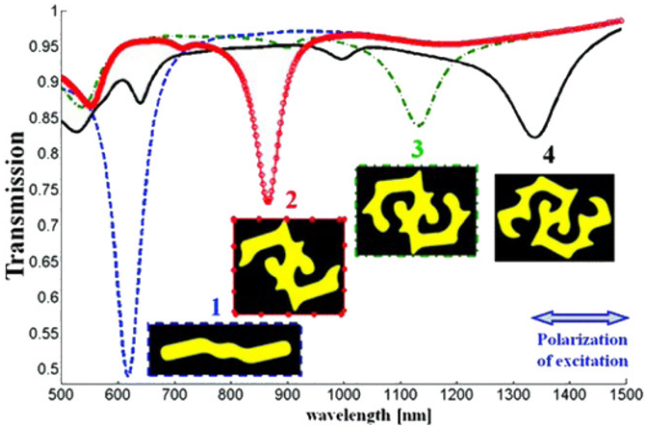


**Figure 8.** Transmission spectra of particles engineered by an evolutionary algorithm. Insets: respective particle shapes: '1' particle, blue dashed line; '2', red circles; '3', green dash–dotted line; '4', black solid line. The arrow shows the polarization of the excitation electrical field. Reproduced with permission from [111]. Copyright 2011 American Physical Society.

evolutionary algorithms have been shown to provide 'on demand' spectral response properties of plasmonic particles and even simultaneously manipulate several quasistatic resonances independently [111].

The proposed method is based on a series of small perturbations applied to an initial particle, which enables the modification of the spectral location of a resonance or even multiple resonances according to specific predetermined values. Small perturbations of an initial particle geometry yield small shifts of its resonances. It may be shown and even analytically proved that a proper sequence of perturbations is capable of shifting the resonances toward the requested values. Figure 8 shows the transmission spectra of a particle series (originated from ellipsoid) with predetermined dipole resonance frequencies constructed by an evolutionary algorithm and verified by FDTD simulation.

### *4.5. Substrate of the nano-antenna*

Resonance of the particle embedded in the homogeneous dielectric medium depends on the dielectric constant of the surroundings, similarly to the dependence derived in condition (1) for a spherical nanoparticle, i.e. for a denser medium the resonance will be moved to the red. However, in most experimental realizations (except for colloidal samples) arrays of plasmonic nanoparticles are fabricated on the top of a dielectric substrate, usually glass or quartz and sometimes semiconductor, with air as a top cladding material. Prediction of the resonance locations and shapes in such an asymmetric configuration is more complicated and challenging, but substrates may be used for resonance tuning and adjustment of the required properties.

The simplest interpretation of substrate action, proposed first by Yamaguchi *et al* [112], provides an explanation by image theory, where additional image charges, coming from the induced polarization in the dielectric substrate, are produced by the plasmonic particle at resonance (figure 9).

According to the polarization of the incident field which excites the plasmon resonance in the nanoparticle, the substrate may enhance (figure 9(a)) or clamp the far field scattering from the particles (figure 9(b)). Additionally, the polarization dependences for particles embedded in a homogeneous medium and for those deposited on a substrate are different, since asymmetry, caused by the substrate, removes the mode degeneracy between 's'- and 'p'-polarizations, thus leading to the split of the resonances for unpolarized illumination [113].

In order to estimate the influence of a substrate quantitatively several models have been proposed. The simplest one is the image dipole model that calculates the interaction between the dipole mode induced in the metal nanoparticle and the dipole of its image screened by the substrate. This model, however, fails for particles of nanometric dimensions in very close proximity to the substrate, since the distance between interacting dipoles will be too short, and multipolar interactions should also be taken into account. An extension of the image model was proposed by Román-Velázquez *et al* [114] who investigated theoretically the multipolar effects on the effective polarizability of a spherical particle lying over a substrate. The effect of multipolar coupling was also measured on alkali-metal particles due to their free-electron character and moderate damping [115]. The accuracy of the multipolar expansion is determined by the truncation of the otherwise infinite series of multipolar terms. On the

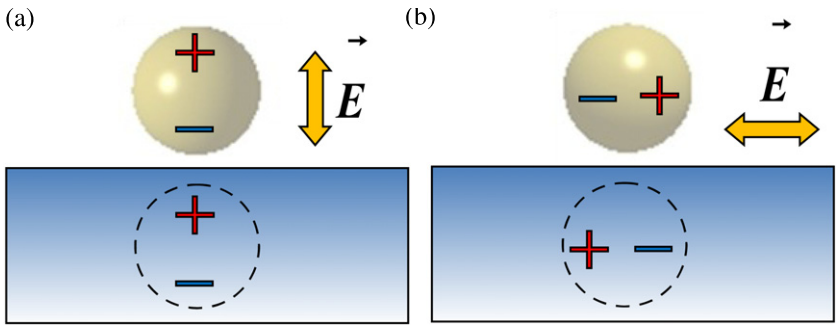


**Figure 9.** Image description of substrate action. Dipole induced resonance perpendicular (a) or parallel (b) to the surface.

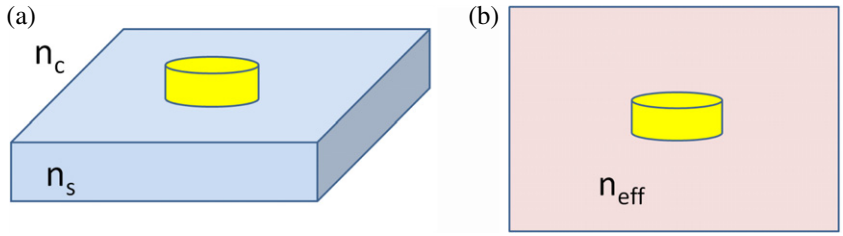


**Figure 10.** Scheme of the effective medium approximation. (a) Particle in an asymmetric configuration with different refractive indices of the substrate $n_s$ and cladding $n_c$. (b) Particle embedded in a homogeneous effective medium $n_{eff}$.

other hand, this accuracy can be increased by using the spheroidal multipole expansion instead of the spherical one. For particle shapes such as disks or needles, the induced charges, although enclosed within the particle's volume, do not occupy it completely. In this case the shape of the radiation can better be described by a flattened or elongated source volume rather than a spherical one. The spheroidal wave expansion [116] is thus a generalization of the spherical wave expansion and it is more appropriate to describe general spheroidal volumes. In the case of simple spherical particles both expansions will of course give the same result. The increase in accuracy by implementation of the spheroidal multipole expansion to describe the interaction between the nanoparticle and its image charge has been shown both theoretically [117] and experimentally [118]. In both works it was shown that spheroidal dipole order was accurate enough whereas for spherical expansion quadrupole and higher terms were required.

'Bright' plasmon modes possess finite dipole moments and can therefore be efficiently excited by incident light even for a standalone particle. But 'dark' modes, such as quadrupole ones, do not couple efficiently to far field light and, generally, do not leave a signature in the transmission spectrum. Symmetry breaking introduced by the substrate allows excitation of 'dark' modes of the original nanoparticle. Moreover, for particles deposited on a substrate, interaction between 'dark' and 'bright' modes becomes possible, giving rise to the appearance of Fano resonances [119, 120] that are significantly more sensitive to the local dielectric environment than the primitive plasmon modes of the nanostructure [121].

While the strength of the image charge is screened by the substrate permittivity and is thus, generally, much weaker than the charge induced in the particle located on this substrate, metallic substrates produce image charges comparable with those in the particle. Therefore the resonances of plasmonic nanoparticles located very close to the metallic substrate will be considerably modified [122] relative to the dielectric case. While metal substrates work as a good mirror, substrates with a moderate imaginary part of permittivity can also influence the plasmon resonance of the nanoparticles, especially the shape of the resonance, emphasizing the importance of substrate absorption [123].

The asymmetry caused by substrates can be reduced by increasing the refractive index of the cladding material. Since the plasmon resonance of a nanostructure is sensitive to the material properties of the whole surroundings it will also be shifted by the gradual change of the cladding refractive index [124, 125]. This property is frequently used for sensor applications.

Interpretation of the interaction between the particle and the supporting substrate by image theory provides significant physical insight into the problem. On the other hand it is sometimes too complicated to enable prediction of the resonance wavelength of the dipole mode of the particle fabricated on a flat substrate relative to the stand alone case. In general, the dependence of the dipole resonance on the substrate refractive index is a simple monotonic function similar to the linear dependence shown in [126]. Such a dependence can be described by using the concept of the effective medium approximation (shown in figure 10).

In this model the resonance frequency of a plasmonic particle on a substrate is similar to that of the particle in a homogeneous effective medium [127].

## 5. Applications of plasmonic nano-antennas

The action of a conventional antenna is either the collection of electromagnetic far field radiation (receiver mode), or direction of radiation to a far field (transmission mode). Plasmonic nano-antennas can be used in a similar way, while additional applications, which stem from the unique abilities of plasmonic nanoparticles to localize electromagnetic radiation on the nanoscale and from their sensitivity to the environment, are imminent.

### *5.1. Receiver mode*

The ability of a plasmonic nano-antenna to be efficiently coupled to far field radiation and to localize it into small volumes can be used in different fields. In the visible range of the spectrum the focusing of incident radiation onto absorbing materials is of great importance for solar cells, as the thicknesses of the absorbing materials may be reduced by improving the absorption efficiency [79]. In the infrared spectrum, where detection of weak signals is challenging because of background noise, enhanced absorption may be employed for improvement of photo-detection. Reduction of the active material volume by improving the absorption within it may significantly improve the signal-to-noise ratio. Dense nanoparticle arrays have been shown to enhance the photocurrent in a 165 nm thick silicon-on-insulator (SOI) photo-detector by a factor of 20 at 800 nm wavelength of

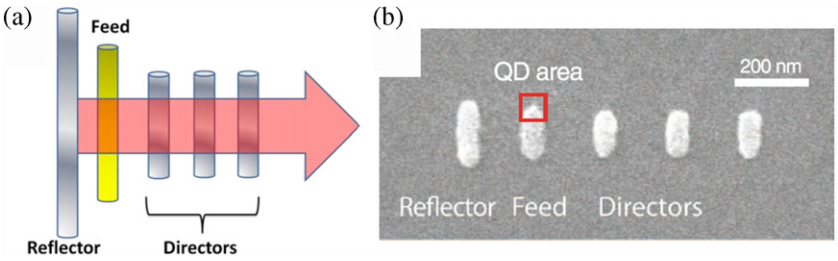


**Figure 11.** (a) Scheme of the Yagi–Uda antenna and (b) the nano Yagi–Uda antenna (reproduced with permission from [136]. Copyright 2010 AAAS).

incident radiation [128]. Improvement of quantum well and dot based detectors has been demonstrated by incorporation of hole arrays [129, 130] and particle lattices [131]. The absorption may be enhanced even at much longer wavelengths (above 10 $\mu$m), where free carriers are playing the key role [132].

An additional very promising and emerging application of plasmonic nanoparticles in the NIR is related to biomedicine and biosensing [24, 25]. Here, the resonant behavior of localized plasmons may be taken toward the single molecule detection limit and for observation of molecular binding events and changes in molecular conformation [133]. So-called 'plasmon rulers' may be used for observation of conformational changes of biomolecules in both *in vitro* and *in vivo* scenarios [134] or even for protein networking [135]. Losses corresponding to plasmonic particles on resonance may be used for medical treatment, where these particles may be selectively attached to desired sites (such as cancer tumors), heated by infrared radiation, and subsequently burn the nearby cells [26, 27].

### 5.2. Transmission mode

Optical emitters have low radiation efficiencies simply because their physical dimensions are small. The basic idea for light extraction from such emitters is to couple them (within their near field) to larger objects, impedance-matched to free space. An additional requirement is directionality—while standalone emitters produce purely uniform radiation, the latter may be shaped by antennas. Counterparts of conventional radio-frequency antennas may be used in optics, e.g. Yagi–Uda (figure 11(a)).

The optical version of the Yagi–Uda antenna is based on coupled particles of carefully designed dimensions and an optical emitter (usually a quantum dot) placed in the vicinity of 'feed' particles (figure 11(b)). The directionality is achieved by blocking the radiation by a 'reflector' in certain directions and beaming by the 'directors' assembly. The optical Yagi–Uda configurations on the nanoscale were recently theoretically and experimentally realized [64, 136–138].

Optical counterparts of fractal antennas, which in principle may be very broadband, have also recently been proposed [139].

Optical beaming of radiation coming from emitting dipoles may also be achieved by surface patterning. Emitters, situated in sub wavelength holes in metal films, emit radiation into plasmons that are coupled to propagating surface plasmon polaritons, which subsequently directionally re-radiate to the far field by periodic Bragg patterns etched in the film [140, 141].

### 5.3. Enhancement of quantum and nonlinear phenomena

The electromagnetic environment may dramatically influence the radiation properties of emitters. Generally, classical antennas are treated in terms of Green's functions (electromagnetic responses for elementary excitations), while Fermi's golden rule with 'density of states' treatment provides, seemingly, more physical intuition in the optical range. However, there is a one-to-one correspondence between the two approaches if the weak coupling regime is considered [142].

The enhancement of the spontaneous emission rates in the environment relative to free space is, generally, described in terms of the Purcell factor [143], given by

$$P = \frac{3Q\,(\lambda_c/n)^3}{4\pi^2 V_{\mathrm{eff}}} \tag{7}$$

where $P$ is the Purcell factor, depending on the cavity quality factor $Q$, the cavity central wavelength $\lambda_c$, the average refractive index $n$, and the effective cavity modal volume $V_{\mathrm{eff}}$.

While the quality factors of plasmonic antennas/cavities are not so high (order of ten), being limited in the quasistatic limit by the ratio of real and imaginary parts of the dielectric permittivity of the cavity [144], the modal volumes of the localized plasmonic modes may go far beyond the diffraction limit [145]. A number of plasmonic cavities with very small modal volumes have been proposed, e.g. with values of $\{Q, V_{\mathrm{eff}}/\lambda^3\}$ of {10, 0.006} [146], {30, 0.015} [147], and {30, 0.0002} [148], giving emission enhancement by 3–5 orders of magnitude.

While various plasmonic cavities have already been discussed, the emitters themselves require separate treatment. It was shown in [149] that the emitters' radiation efficiency should initially be low; otherwise significant plasmonic enhancement will not be obtained. The coupling efficiency of individual quantum emitters is of potential significance for quantum information applications; here plasmonic antennas may yield significant improvement, e.g. plasmonic nanowires, coupled to a single quantum dot, were shown to engineer photon–emitter interactions [150].

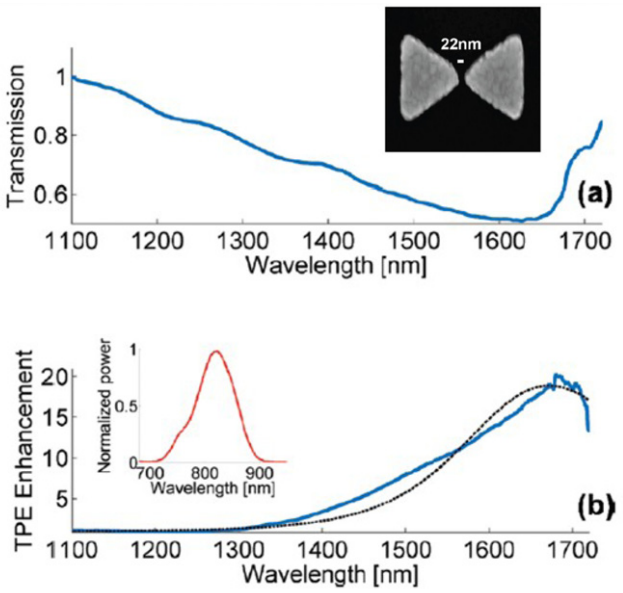


**Figure 12.** (a) Transmission spectrum of the passive bow-tie particle array. The inset is the SEM image of the bow-tie antenna. (b) Spectrum of the enhancement in TPE by the bow-tie array: measurement, solid blue line; FDTD calculation, dashed black line. The inset is the one-photon emission spectrum. Reproduced with permission from [151]. Copyright 2010 American Chemical Society.

Plasmonic cavities may also enhance nonlinear processes such as spontaneous two-photon emission (TPE) at room temperature [151] (shown in figure 12), photoluminescence from quantum wells [152], Raman scattering [153], and other nonlinear phenomena, originating from adjacent nonlinear materials or the metals themselves [154–160].

## 6. Future outlook and conclusion

Phenomena related to localized plasmon resonances are a well proven and fast developing branch of physics. Having a large number of potential applications, some already demonstrated, plasmonic nano-antennas, in particular in the NIR regime, are employed in various disciplines. The unique property of deep sub wavelength confinement of optical fields, corresponding to localized plasmon resonances, may dramatically change the essentials of light–matter interaction and its exploitation.

Comprehensive research has been performed on the subject and much is well understood now—advanced theoretical modes have been developed and many of them have been experimentally proven. However, there are still substantial issues, both technological and conceptual, that are not fully resolved, making the area of plasmonics and, in particular, localized surface plasmon resonances, an evolving and promising niche in physics. Recently, more attention has been devoted to ultra-small particles with dimensions (or interparticle separation distances) smaller than ∼10 nm. From a technological point of view, the repeatable fabrication of such tiny particles is challenging, and most of the techniques, applied straightforwardly, are failing. Other concepts should be developed and applied to reach the above dimensionality. The particular interest in particles smaller than ∼10 nm is due to the fact that the mean free path of room temperature electrons in plasmonic metals is of this order. This means that the bulk properties attributed to the material components are not valid anymore and the dielectric susceptibility model cannot be used in predictions of phenomena and modeling for such small structures. Advanced hydrodynamical models or quantum description of the processes should be applied [161–164]. Specifically, boundaries (and tunneling effects through them) and surface states may play a key role in the optical properties of very small particles, while larger specimens may be treated straightforwardly by applying macroscopic Maxwell equations and proper boundary conditions.

As was already mentioned, a large number of emerging applications are based on, or have a strong component relying on, plasmonic resonances. Here we outline once again the importance of quantum optics and biomedical applications. The unique properties of strong plasmonic localization provide novel solutions to old problems of quantum optics, in particular radiation and collection efficiencies. Insufficient collection efficiencies may result in fundamental limitations for quantum protocols, and existing devices still require significant improvement. Biomedical applications, including cancer treatment in particular, represent another promising niche that implements the localized plasmon resonance in the NIR, and are under considerable study.

## Acknowledgments

We thank our colleagues who have graciously allowed us to reproduce their work here. We also acknowledge the Israeli Ministry of Defense and AFOSR for partial financial support of our research.

P Ginzburg acknowledges the Royal Society for a Newton International Fellowship and Yad Hanadiv for a Rothschild Fellowship.

## References

[1] *Bible* Exodus 32 verses 19-20
[2] Newton S I and Chittenden N W 1848 *Newton's Principia: The Mathematical Principles of Natural Philosophy* D. Adee
[3] Wood R W 1902 On a remarkable case of uneven distribution of light in a diffraction grating spectrum *Phil. Mag. Ser.* 6 **4** 396–402
[4] Ritchie R H 1957 Plasma losses by fast electrons in thin films *Phys. Rev.* **106** 874
[5] Powell C J and Swan J B 1959 Origin of the characteristic electron energy losses in aluminum *Phys. Rev.* **115** 869
[6] Ritchie R H, Arakawa E T, Cowan J J and Hamm R N 1968 Surface-plasmon resonance effect in grating diffraction *Phys. Rev. Lett.* **21** 1530
[7] Kretschmann E and Raether H 1968 Radiative decay of non radiative surface plasmons excited by light (Surface plasma waves excitation by light and decay into photons applied to nonradiative modes) *Z. Naturf.* a **23** 2135
[8] Otto A 1968 Excitation of nonradiative surface plasma waves in silver by the method of frustrated total reflection *Z. Phys.* A **216** 398–410
[9] Lorenz L 1898 Lysbevaegelsen i og uden for en hal plane lysbôlger belyst kulge *Vidensk. Selk. Skr.* **6** 1–62

[10] Mie G 1908 Beiträge zur Optik trüber Medien, speziell kolloidaler Metallösungen *Ann. Phys.* **25** 377

[11] Kreibig U and Zacharias P 1970 Surface plasma resonances in small spherical silver and gold particles *Z. Phys.* A **231** 128–43

[12] Fleischmann M, Hendra P J and McQuillan A J 1974 Raman spectra of pyridine adsorbed at a silver electrode *Chem. Phys. Lett.* **26** 163–6

[13] Ebbesen T W, Lezec H J, Ghaemi H F, Thio T and Wolff P A 1998 Extraordinary optical transmission through sub-wavelength hole arrays *Nature* **391** 667–9

[14] Lezec H J, Degiron A, Devaux E, Linke R A, Martin-Moreno L, Garcia-Vidal F J and Ebbesen T W 2002 Beaming light from a subwavelength aperture *Science* **297** 820–2

[15] Stockman M I 2004 Nanofocusing of optical energy in tapered plasmonic waveguides *Phys. Rev. Lett.* **93** 137404

[16] Ropers C, Neacsu C C, Elsaesser T, Albrecht M, Raschke M B and Lienau C 2007 Grating-coupling of surface plasmons onto metallic tips: a nanoconfined light source *Nano Lett.* **7** 2784–8

[17] Verhagen E, Spasenovicacute M, Polman A and Kuipers L (Kobus) 2009 Nanowire plasmon excitation by adiabatic mode transformation *Phys. Rev. Lett.* **102** 203904

[18] Ginzburg P, Arbel D and Orenstein M 2006 Gap plasmon polariton structure for very efficient microscale-to-nanoscale interfacing *Opt. Lett.* **31** 3288–90

[19] Ginzburg P and Orenstein M 2007 Plasmonic transmission lines: from micro to nano scale with $\lambda/4$ impedance matching *Opt. Express* **15** 6762–7

[20] Krasavin A V and Zayats A V 2007 Passive photonic elements based on dielectric-loaded surface plasmon polariton waveguides *Appl. Phys. Lett.* **90** 211101

[21] Chen L, Shakya J and Lipson M 2006 Subwavelength confinement in an integrated metal slot waveguide on silicon *Opt. Lett.* **31** 2133–5

[22] Nie S and Emory S R 1997 Probing single molecules and single nanoparticles by surface-enhanced Raman scattering *Science* **275** 1102–6

[23] McFarland A D and Van Duyne R P 2003 Single silver nanoparticles as real-time optical sensors with zeptomole sensitivity *Nano Lett.* **3** 1057–62

[24] Haes A J, Hall W P, Chang L, Klein W L and Van Duyne R P 2004 A localized surface plasmon resonance biosensor: first steps toward an assay for Alzheimer's disease *Nano Lett.* **4** 1029–34

[25] Kabashin A V, Evans P, Pastkovsky S, Hendren W, Wurtz G A, Atkinson R, Pollard R, Podolskiy V A and Zayats A V 2009 Plasmonic nanorod metamaterials for biosensing *Nature Mater.* **8** 867–71

[26] Loo C, Lowery A, Halas N, West J and Drezek R 2005 Immunotargeted nanoshells for integrated cancer imaging and therapy *Nano Lett.* **5** 709–11

[27] Loo C, Lin A, Hirsch L, Lee M-H, Barton J, Halas N, West J and Drezek R 2004 Nanoshell-enabled photonics-based imaging and therapy of cancer *Technol. Cancer Res. Treat* **3** 33–40

[28] Engheta N and Ziolkowski R W 2006 *Metamaterials: Physics and Engineering Explorations* (New York: Wiley)

[29] Pollard R J, Murphy A, Hendren W R, Evans P R, Atkinson R, Wurtz G A, Zayats A V and Podolskiy V A 2009 Optical nonlocalities and additional waves in epsilon-near-zero metamaterials *Phys. Rev. Lett.* **102** 127405

[30] Shalaev V M 2007 Optical negative-index metamaterials *Nature Photon.* **1** 41–8

[31] Mirin N A and Halas N J 2009 Light-bending nanoparticles *Nano Lett.* **9** 1255–9

[32] Hill M T, Oei Y-S, Smalbrugge B, Zhu Y, de Vries T, van Veldhoven P J, van Otten F W M, Eijkemans T J, Turkiewicz J P, de Waardt H, Geluk E J, Kwon S-H, Lee Y-H, Notzel R and Smit M K 2007 Lasing in metallic-coated nanocavities *Nature Photon.* **1** 589–94

[33] Stockman M I 2008 Spasers explained *Nature Photon.* **2** 327–9

[34] Wurtz G A and Zayats A V 2008 Nonlinear surface plasmon polaritonic crystals *Laser Photon. Rev.* **2** 125–35

[35] Khurgin J B, Sun G and Soref R A 2007 Enhancement of luminescence efficiency using surface plasmon polaritons: figures of merit *J. Opt. Soc. Am.* B **24** 1968–80

[36] Kneipp K, Wang Y, Kneipp H, Perelman L T, Itzkan I, Dasari R R and Feld M S 1997 Single molecule detection using surface-enhanced Raman scattering (SERS) *Phys. Rev. Lett.* **78** 1667

[37] Tao A, Kim F, Hess C, Goldberger J, He R, Sun Y, Xia Y and Yang P 2003 Langmuir–Blodgett silver nanowire monolayers for molecular sensing using surface-enhanced Raman spectroscopy *Nano Lett.* **3** 1229–33

[38] Ekinci Y, Solak H H and Löffler J F 2008 Plasmon resonances of aluminum nanoparticles and nanorods *J. Appl. Phys.* **104** 083107

[39] Ginzburg P and Orenstein M 2008 Metal-free quantum-based metamaterial for surface plasmon polariton guiding with amplification *J. Appl. Phys.* **104** 063513

[40] Ginzburg P and Orenstein M 2008 Nonmetallic left-handed material based on negative-positive anisotropy in low-dimensional quantum structures *J. Appl. Phys.* **103** 083105

[41] West P R, Ishii S, Naik G V, Emani N K, Shalaev V M and Boltasseva A 2010 Searching for better plasmonic materials *Laser Photon. Rev.* **4** 795–808

[42] Boltasseva A and Atwater H A 2011 Low-loss plasmonic metamaterials *Science* **331** 290–1

[43] Sun Y and Xia Y 2003 Alloying and dealloying processes involved in the preparation of metal nanoshells through a galvanic replacement reaction *Nano Lett.* **3** 1569–72

[44] Chen J, Saeki F, Wiley B J, Cang H, Cobb M J, Li Z-Y, Au L, Zhang H, Kimmey M B, Li X and Xia Y 2005 Gold nanocages: bioconjugation and their potential use as optical imaging contrast agents *Nano Lett.* **5** 473–7

[45] Wang H, Brandl D W, Le F, Nordlander P and Halas N J 2006 Nanorice: a hybrid plasmonic nanostructure *Nano Lett.* **6** 827–32

[46] Nehl C L, Liao H and Hafner J H 2006 Optical properties of star-shaped gold nanoparticles *Nano Lett.* **6** 683–8

[47] McConnell M D, Kraeutler M J, Yang S and Composto R J 2010 Patchy and multiregion janus particles with tunable optical properties *Nano Lett.* **10** 603–9

[48] Chen S and Carroll D L 2002 Synthesis and characterization of truncated triangular silver nanoplates *Nano Lett.* **2** 1003–7

[49] Hao E, Bailey R C, Schatz G C, Hupp J T and Li S 2004 Synthesis and optical properties of 'branched' gold nanocrystals *Nano Lett.* **4** 327–30

[50] Pastoriza-Santos I and Liz-Marzán L M 2002 Synthesis of silver nanoprisms in DMF *Nano Lett.* **2** 903–5

[51] Sun Y, Mayers B and Xia Y 2003 Transformation of silver nanospheres into nanobelts and triangular nanoplates through a thermal process *Nano Lett.* **3** 675–9

[52] Formanek F, Takeyasu N, Tanaka T, Chiyoda K, Ishikawa A and Kawata S 2006 Selective electroless plating to fabricate complex three-dimensional metallic micro/nanostructures *Appl. Phys. Lett.* **88** 083110

[53] Aksu S, Yanik A A, Adato R, Artar A, Huang M and Altug H 2010 High-throughput nanofabrication of infrared plasmonic nanoantenna arrays for vibrational nanospectroscopy *Nano Lett.* **10** 2511–8

[54] Kubo W and Fujikawa S 2011 Au double nanopillars with nanogap for plasmonic sensor *Nano Lett.* **11** 8–15

[55] Boltasseva A and Shalaev V M 2008 Fabrication of optical negative-index metamaterials: recent advances and outlook *Metamaterials* **2** 1–17

[56] Chen W, Abeysinghe D C, Nelson R L and Zhan Q 2010 Experimental confirmation of miniature spiral plasmonic lens as a circular polarization analyzer *Nano Lett.* **10** 2075–9

[57] Mojarad N M and Agio M 2009 Tailoring the excitation of localized surface plasmon-polariton resonances by focusing radially-polarized beams *Opt. Express* **17** 117–22

[58] Ginzburg P, Nevet A, Berkovitch N, Normatov A, Lerman G M, Yanai A, Levy U and Orenstein M 2011 Plasmonic resonance effects for tandem receiving-transmitting nanoantennas *Nano Lett.* **11** 220–4

[59] McFarland A D and Van Duyne R P 2003 Single silver nanoparticles as real-time optical sensors with zeptomole sensitivity *Nano Lett.* **3** 1057–62

[60] van Dijk M A, Lippitz M and Orrit M 2005 Far-field optical microscopy of single metal nanoparticles *Acc. Chem. Res.* **38** 594–601

[61] Schnell M, Garcia-Etxarri A, Huber A J, Crozier K, Aizpurua J and Hillenbrand R 2009 Controlling the near-field oscillations of loaded plasmonic nanoantennas *Nature Photon.* **3** 287–91

[62] Huang J-S, Kern J, Geisler P, Weinmann P, Kamp M, Forchel A, Biagioni P and Hecht B 2010 Mode imaging and selection in strongly coupled nanoantennas *Nano Lett.* **10** 2105–10

[63] Lin H-Y, Huang C-H, Chang C-H, Lan Y-C and Chui H-C 2010 Direct near-field optical imaging of plasmonic resonances in metal nanoparticle pairs *Opt. Express* **18** 165–72

[64] Coenen T, Vesseur E J R, Polman A and Koenderink A F 2011 Directional emission from plasmonic yagi–uda antennas probed by angle-resolved cathodoluminescence spectroscopy *Nano Lett.* **11** 3779–84

[65] Nelayah J, Kociak M, Stephan O, Garcia de Abajo F J, Tence M, Henrard L, Taverna D, Pastoriza-Santos I, Liz-Marzan L M and Colliex C 2007 Mapping surface plasmons on a single metallic nanoparticle *Nature Phys.* **3** 348–53

[66] Bohren C F and Huffman D R 1983 *Absorption and Scattering of Light by Small Particles* vol 1 (New York: Wiley–Interscience)

[67] Cai W, Chettiar U K, Kildishev A V and Shalaev V M 2007 Optical cloaking with metamaterials *Nature Photon.* **1** 224–7

[68] Chu S-T and Chaudhuri S K 1989 A finite-difference time-domain method for the design and analysisof guided-wave optical structures *J. Lightwave Technol.* **7** 2033–8

[69] Oubre C and Nordlander P 2004 Optical properties of metallodielectric nanostructures calculated using the finite difference time domain method *J. Phys. Chem.* B **108** 17740–7

[70] Rahman B M, Fernandez F A and Davies J B 1991 Review of finite element methods for microwave and opticalwaveguides *Proc. IEEE* **79** 1442–8

[71] García de Abajo F J and Howie A 1998 Relativistic electron energy loss and electron-induced photon emission in inhomogeneous dielectrics *Phys. Rev. Lett.* **80** 5180

[72] Mackowski D W and Mishchenko M I 1996 Calculation of the T matrix and the scattering matrix for ensembles of spheres *J. Opt. Soc. Am.* A **13** 2266–78

[73] Yurkin M A and Hoekstra A G 2007 The discrete dipole approximation: an overview and recent developments *J. Quant. Spectrosc. Radiat. Transfer* **106** 558–89

[74] Xu Y-l 1995 Electromagnetic scattering by an aggregate of spheres *Appl. Opt.* **34** 4573–88

[75] Myroshnychenko V, Rodríguez-Fernández J, Pastoriza-Santos I, Funston A M, Novo C, Mulvaney P, Liz-Marzán L M and García de Abajo F J 2008 Modelling the optical response of gold nanoparticles *Chem. Soc. Rev.* **37** 1792

[76] Khlebtsov B N and Khlebtsov N G 2007 Multipole plasmons in metal nanorods: scaling properties and dependence on particle size, shape, orientation, and dielectric environment *J. Phys. Chem.* C **111** 11516–27

[77] Bryant G W, Garcia de Abajo F J and Aizpurua J 2008 Mapping the plasmon resonances of metallic nanoantennas *Nano Lett.* **8** 631–6

[78] Zuloaga J, Prodan E and Nordlander P 2010 Quantum plasmonics: optical properties and tunability of metallic nanorods *ACS Nano* **4** 5269–76

[79] Atwater H A and Polman A 2010 Plasmonics for improved photovoltaic devices *Nature Mater.* **9** 205–13

[80] Diukman I, Tzabari L, Berkovitch N, Tessler N and Orenstein M 2011 Controlling absorption enhancement in organic photovoltaic cells by patterning Au nano disks within the active layer *Opt. Express* **19** A64–71

[81] Prodan E and Nordlander P 2004 Plasmon hybridization in spherical nanoparticles *J. Chem. Phys.* **120** 5444

[82] Prodan E, Radloff C, Halas N J and Nordlander P 2003 A hybridization model for the plasmon response of complex nanostructures *Science* **302** 419–22

[83] Nordlander P, Oubre C, Prodan E, Li K and Stockman M I 2004 Plasmon hybridization in nanoparticle dimers *Nano Lett.* **4** 899–903

[84] Brongersma M L, Hartman J W and Atwater H A 2000 Electromagnetic energy transfer and switching in nanoparticle chain arrays below the diffraction limit *Phys. Rev.* B **62** R16356

[85] Maier S A, Brongersma M L, Kik P G, Meltzer S, Requicha A A, Koel B E and Atwater H A 2003 Plasmonics—a route to nanoscale optical devices *Adv. Mater.* **15** 562–2

[86] Sweatlock L A, Maier S A, Atwater H A, Penninkhof J J and Polman A 2005 Highly confined electromagnetic fields in arrays of strongly coupled Ag nanoparticles *Phys. Rev.* B **71** 235408

[87] Maier S A, Kik P G, Atwater H A, Meltzer S, Harel E, Koel B E and Requicha A A G 2003 Local detection of electromagnetic energy transport below the diffraction limit in metal nanoparticle plasmon waveguides *Nature Mater.* **2** 229–32

[88] Alù A and Engheta N 2009 Guided propagation along quadrupolar chains of plasmonic nanoparticles *Phys. Rev.* B **79** 235412

[89] Kottmann J P and Martin O J F 2001 Retardation-induced plasmon resonances in coupled nanoparticles *Opt. Lett.* **26** 1096–8

[90] Weber W H and Ford G W 2004 Propagation of optical excitations by dipolar interactions in metal nanoparticle chains *Phys. Rev.* B **70** 125429

[91] Alù A and Engheta N 2008 Input impedance, nanocircuit loading, and radiation tuning of optical nanoantennas *Phys. Rev. Lett.* **101** 043901

[92] Locatelli A, De Angelis C, Modotto D, Boscolo S, Sacchetto F, Midrio M, Capobianco A-D, Pigozzo F M and Someda C G 2009 Modeling of enhanced field confinement and scattering by optical wire antennas *Opt. Express* **17** 16792–800

[93] Alù A, Salandrino A and Engheta N 2006 Negative effective permeability and left-handed materials at optical frequencies *Opt. Express* **14** 1557–67

[94] Fung K H and Chan C T 2008 Analytical study of the plasmonic modes of a metal nanoparticle circular array *Phys. Rev.* B **77** 205423

[95] Hentschel M, Dregely D, Vogelgesang R, Giessen H and Liu N 2011 Plasmonic oligomers: the role of individual particles in collective behavior *ACS Nano* **5** 2042–50

[96] Lassiter J B, Sobhani H, Fan J A, Kundu J, Capasso F, Nordlander P and Halas N J 2010 Fano resonances in plasmonic nanoclusters: geometrical and chemical tunability *Nano Lett.* **10** 3184–9

[97] Lassiter J B, Aizpurua J, Hernandez L I, Brandl D W, Romero I, Lal S, Hafner J H, Nordlander P and Halas N J 2008 Close encounters between two nanoshells *Nano Lett.* **8** 1212–8

[98] Atay T, Song J-H and Nurmikko A V 2004 Strongly interacting plasmon nanoparticle pairs: from dipole–dipole interaction to conductively coupled regime *Nano Lett.* **4** 1627–31

[99] Romero I, Aizpurua J, Bryant G W and García De Abajo F J 2006 Plasmons in nearly touching metallic nanoparticles: singular response in the limit of touching dimers *Opt. Express* **14** 9988–99

[100] Pe'rez-Gonza'lez O, Zabala N, Borisov A G, Halas N J, Nordlander P and Aizpurua J 2010 Optical spectroscopy of conductive junctions in plasmonic cavities *Nano Lett.* **10** 3090–5

[101] Large N, Abb M, Aizpurua J and Muskens O L 2010 Photoconductively loaded plasmonic nanoantenna as building block for ultracompact optical switches *Nano Lett.* **10** 1741–6

[102] Berkovitch N and Orenstein M 2011 Thin wire shortening of plasmonic nanoparticle dimers: the reason for red shifts *Nano Lett.* **11** 2079–82

[103] Mayergoyz I D, Fredkin D R and Zhang Z 2005 Electrostatic (plasmon) resonances in nanoparticles *Phys. Rev.* B **72** 155412

[104] Berkovitch N, Ginzburg P and Orenstein M 2010 Concave plasmonic particles: broad-band geometrical tunability in the near-infrared *Nano Lett.* **10** 1405–8

[105] Rockstuhl C, Lederer F, Etrich C, Zentgraf T, Kuhl J and Giessen H 2006 On the reinterpretation of resonances in split-ring-resonators at normal incidence *Opt. Express* **14** 8827–36

[106] Corrigan T D, Kolb P W, Sushkov A B, Drew H D, Schmadel D C and Phaneuf R J 2008 Optical plasmonic resonances in split-ring resonator structures: an improved LC model *Opt. Express* **16** 19850–64

[107] Holland J H 1992 Genetic algorithms *Sci. Am.* **267** 66–72

[108] Aeschlimann M, Bauer M, Bayer D, Brixner T, García de Abajo F J, Pfeiffer W, Rohmer M, Spindler C and Steeb F 2007 Adaptive subwavelength control of nano-optical fields *Nature* **446** 301

[109] Boag A, Michielssen E and Mittra R 1996 Design of electrically loaded wire antennas using genetic algorithms *IEEE Trans. Antennas Propag.* **44** 687

[110] Forestiere C, Donelli M, Walsh G F, Zeni E, Miano G and Dal Negro L 2010 Particle-swarm optimization of broadband nanoplasmonic arrays *Opt. Lett.* **35** 133–5

[111] Ginzburg P, Berkovitch N, Nevet A, Shor I and Orenstein M 2011 Resonances on-demand for plasmonic nano-particles *Nano Lett.* **11** 2329–33

[112] Yamaguchi T, Yoshida S and Kinbara A 1974 Optical effect of the substrate on the anomalous absorption of aggregated silver films *Thin Solid Films* **21** 173–87

[113] Knight M W, Wu Y, Lassiter J B, Nordlander P and Halas N J 2009 Substrates matter: influence of an adjacent dielectric on an individual plasmonic nanoparticle *Nano Lett.* **9** 2188–92

[114] Román-Velázquez C E, Noguez C and Barrera R G 2000 Substrate effects on the optical properties of spheroidal nanoparticles *Phys. Rev.* B **61** 10427

[115] Beitia C, Borensztein Y, Lazzari R, Nieto J and Barrera R G 1999 Substrate-induced multipolar resonances in supported free-electron metal spheres *Phys. Rev.* B **60** 6018

[116] Flammer C 1957 *Spheroidal Wave Functions* (Palo Alto: Stanford University Press)

[117] Bobbert P A and Vlieger J 1987 The polarizability of a spheroidal particle on a substrate *Physica* A **147** 115–41

[118] Valamanesh M, Borensztein Y, Langlois C and Lacaze E 2011 Substrate effect on the plasmon resonance of supported flat silver nanoparticles *J. Phys. Chem.* C **115** 2914–22

[119] Sherry L J, Chang S-H, Schatz G C, Van Duyne R P, Wiley B J and Xia Y 2005 Localized surface plasmon resonance spectroscopy of single silver nanocubes *Nano Lett.* **5** 2034–8

[120] Zhang S, Bao K, Halas N J, Xu H and Nordlander P 2011 Substrate-induced fano resonances of a plasmonic nanocube: a route to increased-sensitivity localized surface plasmon resonance sensors revealed *Nano Lett.* **11** 1657–63

[121] Hao F, Sonnefraud Y, Dorpe P V, Maier S A, Halas N J and Nordlander P 2008 Symmetry breaking in plasmonic nanocavities: subradiant LSPR sensing and a tunable fano resonance *Nano Lett.* **8** 3983–8

[122] Yamamoto N, Ohtani S and Garci'a de Abajo F J 2011 Gap and mie plasmons in individual silver nanospheres near a silver surface *Nano Lett.* **11** 91–5

[123] Xu G, Chen Y, Tazawa M and Jin P 2006 Influence of dielectric properties of a substrate upon plasmon resonance spectrum of supported Ag nanoparticles *Appl. Phys. Lett.* **88** 043114

[124] Mock J J, Smith D R and Schultz S 2003 Local refractive index dependence of plasmon resonance spectra from individual nanoparticles *Nano Lett.* **3** 485–91

[125] Murray W A, Auguié B and Barnes W L 2009 Sensitivity of localized surface plasmon resonances to bulk and local changes in the optical environment *J. Phys. Chem.* C **113** 5120–5

[126] Duval Malinsky M, Kelly K L, Schatz G C and Van Duyne R P 2001 Nanosphere lithography: effect of substrate on the localized surface plasmon resonance spectrum of silver nanoparticles *J. Phys. Chem.* B **105** 2343–50

[127] Vernon K C, Funston A M, Novo C, Gómez D E, Mulvaney P and Davis T J 2010 Influence of particle–substrate interaction on localized plasmon resonances *Nano Lett.* **10** 2080–6

[128] Stuart H R and Hall D G 1998 Island size effects in nanoparticle-enhanced photodetectors *Appl. Phys. Lett.* **73** 3815

[129] Chang C-C, Sharma Y D, Kim Y-S, Bur J A, Shenoi R V, Krishna S, Huang D and Lin S-Y 2010 A surface plasmon enhanced infrared photodetector based on InAs quantum dots *Nano Lett.* **10** 1704–9

[130] Wu W, Bonakdar A and Mohseni H 2010 Plasmonic enhanced quantum well infrared photodetector with high detectivity *Appl. Phys. Lett.* **96** 161107

[131] Shenoi R V, Rosenberg J, Vandervelde T E, Painter O J and Krishna S 2010 Multispectral quantum dots-in-a-well infrared detectors using plasmon assisted cavities *IEEE J. Quantum Electron.* **46** 1051–7

[132] Shishodia M S, Jayaweera P V V, Matsik S G, Perera A G U, Liu H C and Buchanan M 2011 Surface plasmon enhanced IR absorption: design and experiment *Photon. Nanostruct.- Fundam. Appl.* **9** 95–100

[133] Anker J N, Hall W P, Lyandres O, Shah N C, Zhao J and Van Duyne R P 2008 Biosensing with plasmonic nanosensors *Nature Mater.* **7** 442–53
[134] Jun Y-W, Sheikholeslami S, Hostetter D R, Tajon C, Craik C S and Alivisatos A P 2009 Continuous imaging of plasmon rulers in live cells reveals early-stage caspase-3 activation at the single-molecule level *Proc. Natl Acad. Sci.* **106** 17735–40
[135] Fruhwirth G O, Fernandes L P, Weitsman G, Patel G, Kelleher M, Lawler K, Brock A, Poland S P, Matthews D R, Kéri G, Barber P R, Vojnovic B, Ameer-Beg S M, Coolen A C C, Fraternali F and Ng T 2011 How Förster resonance energy transfer imaging improves the understanding of protein interaction networks in cancer biology *ChemPhysChem* **12** 442–61
[136] Curto A G, Volpe G, Taminiau T H, Kreuzer M P, Quidant R and van Hulst N F 2010 Unidirectional emission of a quantum dot coupled to a nanoantenna *Science* **329** 930–3
[137] Kosako T, Kadoya Y and Hofmann H F 2010 Directional control of light by a nano-optical Yagi-Uda antenna *Nature Photon.* **4** 312–5
[138] Maksymov I S, Davoyan A R and Kivshar Y S 2011 Enhanced emission and light control with tapered plasmonic nanoantennas arXiv:1104.4865
[139] Sederberg S and Elezzabi A Y 2011 Sierpiński fractal plasmonic antenna: a fractal abstraction of the plasmonic bowtie antenna *Opt. Express* **19** 10456–61
[140] Aouani H, Mahboub O, Devaux E, Rigneault H, Ebbesen T W and Wenger J 2011 Plasmonic antennas for directional sorting of fluorescence emission *Nano Lett.* **11** 2400–6
[141] Jun Y C, Huang K C Y and Brongersma M L 2011 Plasmonic beaming and active control over fluorescent emission *Nature Commun.* **2** 283
[142] Novotny L and Hecht B 2006 *Principles of Nano-Optics* (Cambridge: Cambridge University Press)
[143] Purcell E M, Torrey H C and Pound R V 1946 Resonance absorption by nuclear magnetic moments in a solid *Phys. Rev.* **69** 37
[144] Maier S A 2005 Plasmonics—towards subwavelength optical devices *Curr. Nanosci.* **1** 17–22
[145] Gramotnev D K and Bozhevolnyi S I 2010 Plasmonics beyond the diffraction limit *Nature Photon.* **4** 83–91
[146] Miyazaki H T and Kurokawa Y 2006 Squeezing visible light waves into a 3 nm-thick and 55 nm-long plasmon cavity *Phys. Rev. Lett.* **96** 097401
[147] Maier S A 2006 Effective mode volume of nanoscale plasmon cavities *Opt. Quantum. Electron* **38** 257–67
[148] Feigenbaum E and Orenstein M 2008 Ultrasmall volume plasmons, yet with complete retardation effects *Phys. Rev. Lett.* **101** 163902
[149] Biteen J S, Lewis N S, Atwater H A, Mertens H and Polman A 2006 Spectral tuning of plasmon-enhanced silicon quantum dot luminescence *Appl. Phys. Lett.* **88** 131109
[150] Akimov A V, Mukherjee A, Yu C L, Chang D E, Zibrov A S, Hemmer P R, Park H and Lukin M D 2007 Generation of single optical plasmons in metallic nanowires coupled to quantum dots *Nature* **450** 402–6
[151] Nevet A, Berkovitch N, Hayat A, Ginzburg P, Ginzach S, Sorias O and Orenstein M 2010 Plasmonic nanoantennas for broad-band enhancement of two-photon emission from semiconductors *Nano Lett.* **10** 1848–52
[152] Arbel D, Berkovitch N, Nevet A, Peer A, Cohen S, Ritter D and Orenstein M 2011 Light emission rate enhancement from InP MQW by plasmon nano-antenna arrays *Opt. Express* **19** 9807–13
[153] Michaels A M, Jiang J and Brus L 2000 Ag Nanocrystal junctions as the site for surface-enhanced Raman scattering of single rhodamine 6G molecules *J. Phys. Chem.* B **104** 11965–71
[154] Muskens O L, Giannini V, Sánchez-Gil J A and Gómez Rivas J 2007 Strong enhancement of the radiative decay rate of emitters by single plasmonic nanoantennas *Nano Lett.* **7** 2871–5
[155] Tsutsui Y, Hayakawa T, Kawamura G and Nogami M 2011 Tuned longitudinal surface plasmon resonance and third-order nonlinear optical properties of gold nanorods *Nanotechnology* **22** 275203
[156] Fan W, Zhang S, Panoiu N-C, Abdenour A, Krishna S, Osgood R M, Malloy K J and Brueck S R J 2006 Second harmonic generation from a nanopatterned isotropic nonlinear material *Nano Lett.* **6** 1027–30
[157] Danckwerts M and Novotny L 2007 Optical frequency mixing at coupled gold nanoparticles *Phys. Rev. Lett.* **98** 026104
[158] Pu Y, Grange R, Hsieh C-L and Psaltis D 2010 Nonlinear optical properties of core–shell nanocavities for enhanced second-harmonic generation *Phys. Rev. Lett.* **104** 207402
[159] Banaee M G and Crozier K B 2011 Mixed dimer double-resonance substrates for surface-enhanced Raman spectroscopy *ACS Nano* **5** 307–14
[160] Ginzburg P, Hayat A, Berkovitch N and Orenstein M 2010 Nonlocal ponderomotive nonlinearity in plasmonics *Opt. Lett.* **35** 1551–3
[161] Boardman A D 1982 *Electromagnetic Surface Modes* (New York: Wiley)
[162] García de Abajo F J 2008 Nonlocal effects in the plasmons of strongly interacting nanoparticles, dimers, and waveguides *J. Phys. Chem.* C **112** 17983–7
[163] McMahon J M, Gray S K and Schatz G C 2009 Nonlocal optical response of metal nanostructures with arbitrary shape *Phys. Rev. Lett.* **103** 097403
[164] McMahon J M, Gray S K and Schatz G C 2010 Optical properties of nanowire dimers with a spatially nonlocal dielectric function *Nano Lett.* **10** 3473–81